

# Effects of Shear Stress in Teletaction and Human Perception \*

G. Moy and R.S. Fearing  
Department of EE&CS  
University of California  
Berkeley, CA 94720-1770

## Abstract

*Ideally, a tactile stimulator presents information through control of surface normal stress and surface shear stresses. Psychophysical experiments measured the effect of shear stress information on perception of static stimuli. Wax gratings in two different orientations and various spatial frequencies were used as stimuli. Elastic layers, which represent the anti-aliasing filter on a tactile display, were placed over the stimuli. Using an elastic layer which reduces shear stress information transmission did not degrade spatial resolution, but rather, improved perception. Spatial resolution differences due to different elastic layers are explained by modulation indices determined from the predicted sub-surface strain using an elastic half-plane model.*

## 1 Introduction

Information about texture, local compliance, or local shape is important in applications such as telesurgery or handling of fragile objects in telerobotics. Fig. 1 shows a general configuration of a teletaction system. One possible configuration on a robotic laparoscopic telesurgery system. The tactile sensor is mounted on the end effector (the laparoscopic instrument), and the tactile stimulator display is mounted on the master manipulator (the user interface). The tactile stimulator would present information recorded by the tactile sensor to the user. Ideally, the patterns felt by the user would be indistinguishable from direct contact with the environment. The tactile stimulator needs to generate surface stresses that realistically represent data collected by the tactile sensor. To fully control surface stress, the tactile display system should be an array of 3 DOF actuators.

Tactile displays can produce either displacements or forces. In a displacement display, an array of pins are shaped into a contour. In a force display, the pin array will produce a surface stress distribution representing the data. In either case, we examine the effects of reducing the amount of shear stress information transmission. As seen in the Sensopad<sup>1</sup>, a device to aid in breast self examinations, reduction of the shear stress can enhance detection of embedded objects.

Most tactile display systems use an array of actuated 1 DOF pins to stimulate the slowly adapting afferent units. The density of the stimulator array is limited by actuator size. Currently, the spacing between the centers of the pins is around 2 mm [Cohn et al 1992; Howe et al 1995]. The array is covered by an elastic layer which functions as an anti-aliasing filter. Without the anti-aliasing filter, the user would feel an array of pins instead of smooth continuous surfaces. Until actuator technology advances to the point where pin density equals mechanoreceptor density, an anti-aliasing filter will still be needed. When actuator densities are high enough, an elastic layer will be needed to protect users from the small pins stabbing into the skin.

Tactile display designs have used solenoids [Fischer et al, 1995], shape memory alloy [Howe et al 1995; Hasser and Daniels 1996], and pneumatics [Cohn et al 1992]. Electrocutaneous stimulation [Kaczmarek et al 1991] is mechanically quite simple; however, the perceptual effects are hard to analyze. Human tactile perception is not as well understood as the human vision system. Some areas, such as human tactile sensing sensitivity, sensor density, and spatial and temporal frequency response have been studied [Lederman 1978; Phillips and Johnson 1981; Loomis and Lederman 1986; Shimojo et al 1997; Tan 1995; Singh 1997].

The teletaction problem can be split into three parts, a sensor side, a stimulator side, and a communications channel (Figure 2). The communications channel is replaced with direct contact between the sensor and stimulator to avoid aliasing problems. The sensor is represented by one elastic layer, and the display is represented by another elastic layer. With elastic layers between the stimuli and fingertip, we test two different configurations of elastic layers to see if transmission of shear stress affects the perception of grating orientation. One of the elastic layers consists of two 1mm thick pieces of silicone rubber (Dow Corning's HSII). This represents full normal and shear stress information transmission between the tactile sensor and display. The other elastic layer consists of two 1mm thick pieces of HSII with a thin layer of lubricant between them. This represents full normal and reduced shear stress information transmission between the tactile sensor and display. Testing human perception of spatially varied stimuli will determine

\*This work was funded in part by: NSF grant IRI-9531837.

<sup>1</sup>Inventive Products, Inc.



Figure 1: A block diagram representation of a teletaction system.

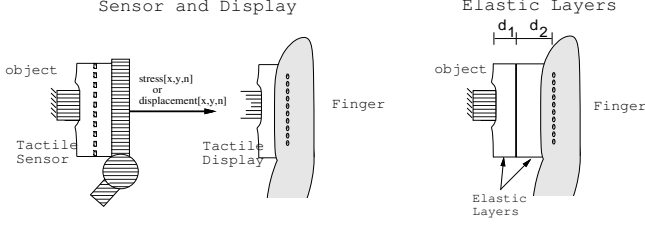


Figure 2: Teletaction with a) a sensor and display, b) elastic layers

whether or not an array of 1 DOF actuators should be as effective as an array of 3 DOF actuators in presenting a normal stress pattern.

## 2 Models of the human finger and stimuli

In this section, we describe a model of the interactions between the human finger and a normally indented stimuli. For simplicity, we use the plane-stress approximation (Figure 3a). Higher order and more realistic models of the finger are being developed by others, such as [Srinivasan and Dandekar 1997]. We first present the geometry and mechanics of the system. We then represent the system as a block diagram.

### 2.1 Model of the Teletaction System

For the teletaction problem we are studying, stimuli are transmitted through two rubber layers to the finger. The two rubber layers represent the tactile sensor and display (Figure 2). We want to model the normal strain due to indentations from the stimuli with the two differing rubber layers. In the first case, the rubber layer is two 1 mm sheets of rubber. The block diagram for the first case is represented in Figure 4a. In the second case, we use two 1 mm sheets of rubber with a lubricant in between the layers, and is represented in Figure 4b. This lubricant has the effect of reducing (and in the ideal case, zeroing) the shear stress from the first layer to the second layer.

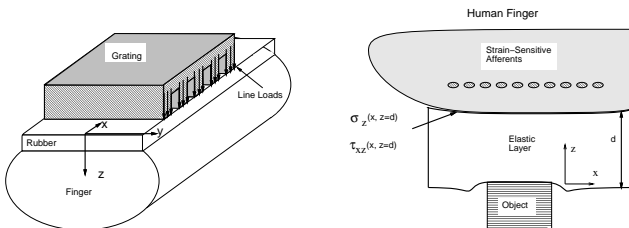


Figure 3: a) Finger and stimuli geometry for plane stress assumption b) slice of the x-z plane

For a basic model of the sensor, stimulator, and finger, we use the half-plane elastic analysis of Phillips and Johnson [1981] as a starting point. The plane stress assumption is used for our analysis since it correlates better with the response of mechanoreceptors in the fingers of macaque monkeys [Phillips and Johnson 1981].

The indentations presented to the finger by the stimuli are represented as line loads applied to the rubber layer. These line loads are constant along the y-axis, but vary along the x-axis. For planar stress analysis, we take a thin slice from the x-z plane, as shown in Figure 3b.

Starting with the stresses in a slice for a normal line load applied at the surface [Johnson 1985] and following the same analysis as [Fearing et al 1997], the normal strain at depth  $z$  due to a line load with normal component  $P$  and tangential component  $Q$  is:

$$\begin{aligned} \epsilon_z &= \epsilon_{zp} + \epsilon_{zq} = \frac{1}{E}(\sigma_z - \nu\sigma_x) + \frac{1}{E}(\sigma_z - \nu\sigma_x) \\ &= \frac{-2Pz}{\pi Er^4}(z^2 - \nu x^2) + \frac{-2Qxz}{\pi Er^4}(z - \nu x) \\ &= \frac{-2z}{\pi Er^4}(P(z^2 - \nu x^2) + Q(xz - \nu x^2)) \end{aligned}$$

This is not what the human measures, but is easily to mathematically compute, and is a good first order approximation.

We assume a normal frictionless indentation, so  $\tau_{xz}(x) = 0$  at the contact surface. The relations of the blocks from Figure 4 based on line load equations from [Fearing, Moy, Tan] are as follows:

$$\begin{aligned} h_{zz}(x) &= \frac{-2z^3}{\pi r^4}, H_{zz}(s) = -2\pi z e^{-2\pi z s} \left( \frac{1}{2\pi z} + s \right), \\ h_{xz}(x) &= \frac{-2x^2 z}{\pi r^4}, H_{xz}(s) = -2\pi z e^{-2\pi z s} \left( \frac{1}{2\pi z} - s \right), \\ h_{\tau z}(x) &= \frac{-2xz^2}{\pi r^4}, H_{\tau z}(s) = j2\pi z s e^{-2\pi z s}, \\ h_{z\tau}(x) &= \frac{-2xz^2}{\pi r^4}, H_{z\tau}(s) = j2\pi z s e^{-2\pi z s}, \\ h_{x\tau}(x) &= \frac{-2x^2 z}{\pi r^4}, H_{x\tau}(s) = j(2 - 2\pi z s) e^{-2\pi z s}, \end{aligned}$$

where  $z$  is the depth of interest,  $s$  is the spatial frequency and is  $\geq 0$ , and  $r^2 = x^2 + z^2$ .

From the block diagrams and relations, transfer functions are calculated for both systems. With no lubricant between the rubber layers (shear stress information transmitted), the overall frequency response for the teletaction system is:

$$\begin{aligned} H_s(s) &= \frac{\mathcal{F}[\epsilon_z(x, z = d_1 + d_2)]}{\mathcal{F}[\sigma_z(x, z = 0)]} \\ &= \frac{1}{E} e^{-2\pi(d_1 + d_2)s} \left( \frac{1}{2} + 3\pi(d_1 + d_2)s \right) \end{aligned}$$

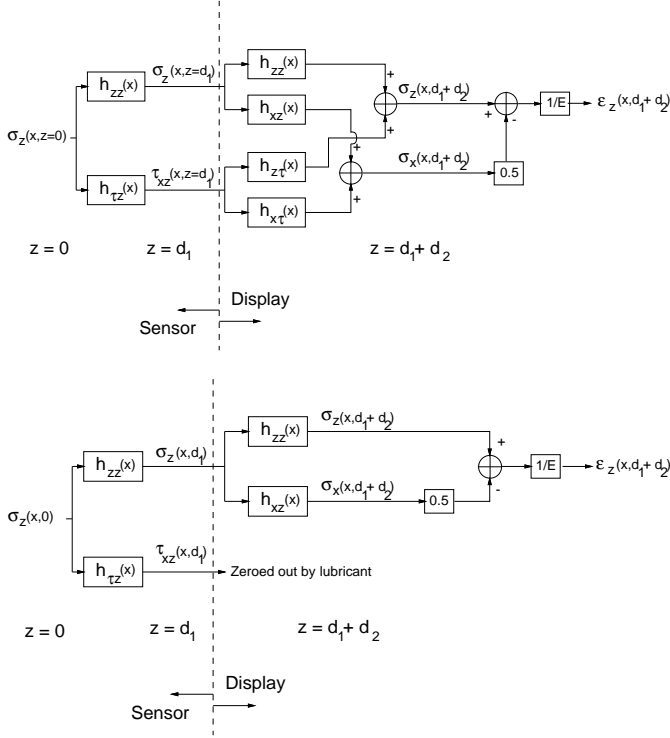


Figure 4: Block diagram representation of the system with two 1 mm sheets of rubber with a) no lubricant, b) a lubricant in between the rubber layers

With lubricant between the rubber layers (no shear stress information transmitted), the overall frequency response for the teletaction system is:

$$\begin{aligned}
 H_{ns}(s) &= \frac{\epsilon_z(x, z = d_1 + d_2)}{\sigma_z(x, z = 0)} \\
 &= \frac{1}{E} e^{-2\pi(d_1+d_2)s} \left( \frac{1}{2} + \pi(d_1 + 3d_2)s \right. \\
 &\quad \left. + 6\pi^2 d_1 d_2 s^2 \right)
 \end{aligned}$$

In our case, we set  $d_1 = 1.0$  mm and  $d_2 = 1.7$  mm (1.0 mm for the second rubber layer and 0.7 mm for the depth of the mechanoreceptors in the skin). The frequency responses are plotted in Figure 5.

## 2.2 Normal Strain Profile based on Displacement Profiles

The systems from section 2.1 predicts the normal strain profile given the input normal stress profile. Since we actually have a displacement profile input from the gratings, we need to find the equivalent set of line loads corresponding to a given displacement profile. We follow the procedure of Phillips and Johnson [1981] as detailed in the Appendix.

Given a deflection profile corresponding to a 4.0 mm period grating indenting 2.0 mm, as shown in Figure 6a, we calculate a line load profile that would produce this deflection profile. Knowing that the normal

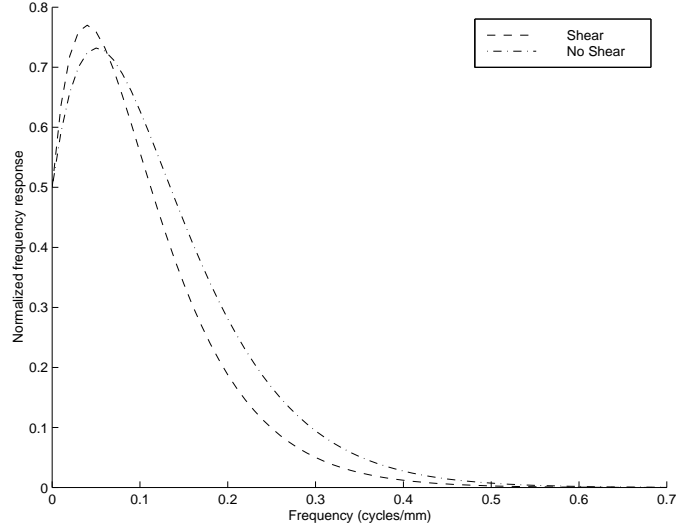


Figure 5: Frequency responses when  $d_1 = 1.0$  mm and  $d_2 = 1.7$  mm

stress should be zero where there is no contact with the grating, and limiting our surface normal stress to only have compressive components, we are left with a surface normal stress profile,  $\sigma_z(x)$ , shown in Figure 6b. The deflection profile corresponding to  $\sigma_z(x)$  can be found by convolving  $\sigma_z(x)$  and  $c(x)$ , as defined in the Appendix, and is shown in Figure 6c.

From the surface normal stress, we can calculate the normal strain profile,  $\epsilon_z(s)$ , for the two different systems shown in Figures 4. A modulation index is calculated for each of the normal strain profiles. The normal strain profile from -10 mm to 10 mm (to avoid the edge effects) can be approximately represented as

$$\epsilon_z(x) \sim \alpha(1 + \mu \cos(\omega x))$$

where  $\alpha$  is a scaling constant,  $\omega$  is the frequency of the grating, and  $\mu$  is the modulation index. The two normal strain profiles are shown in Figure 7. As predicted by Figure 5, the modulation index when no shear information is transmitted is higher than when shear information is transmitted. Figure 8 shows the modulation indices as a function of the grating frequency used as the input. We assume that each subject has a threshold modulation index. Any grating that has a higher modulation index will be perceived. Theoretically, at a sufficiently high modulation index, all subjects should be able to perfectly discriminate orientations. With lubricated elastic layers, we predict that gratings of the same period will have a higher modulation index. If the increase in modulation index crosses the subject's threshold, then orientation discrimination should be greater than chance. Thus, with lubricated elastic layers, higher frequency gratings should be detected.

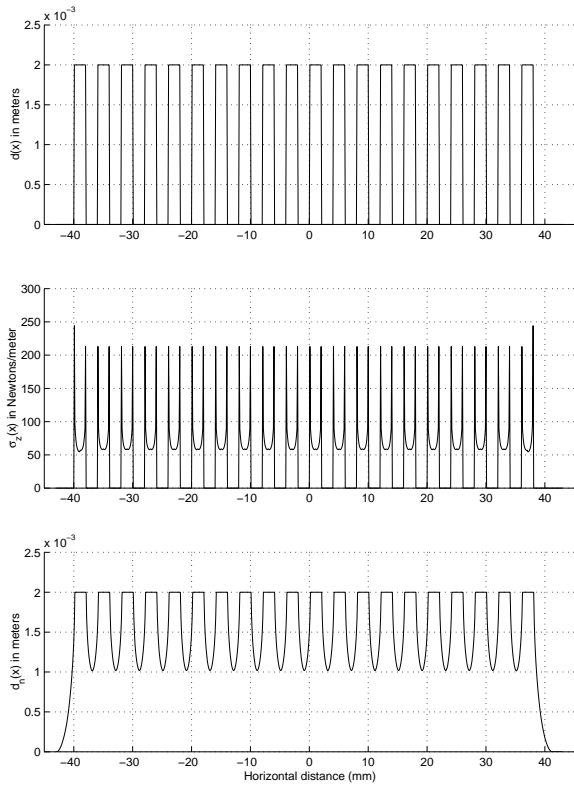


Figure 6: a) Displacement profile applied, b) Surface normal stress, and c) Displacement profile calculated by convolving normal stress in b) with  $c(x)$  in Figure 13

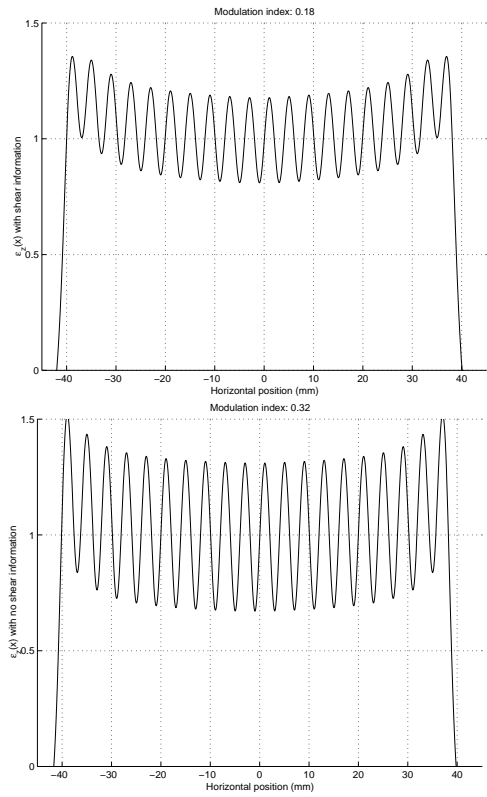


Figure 7: The two normalized normal strains and modulation indices at a depth of 2.7 mm due to a 4.0 mm periodic grating pattern

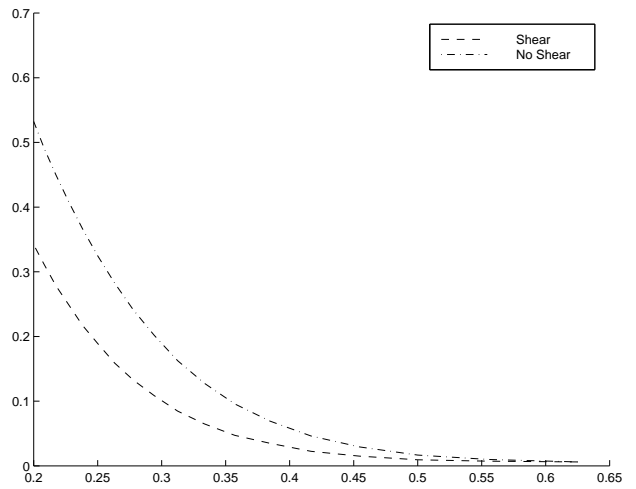


Figure 8: Modulation index vs. frequency

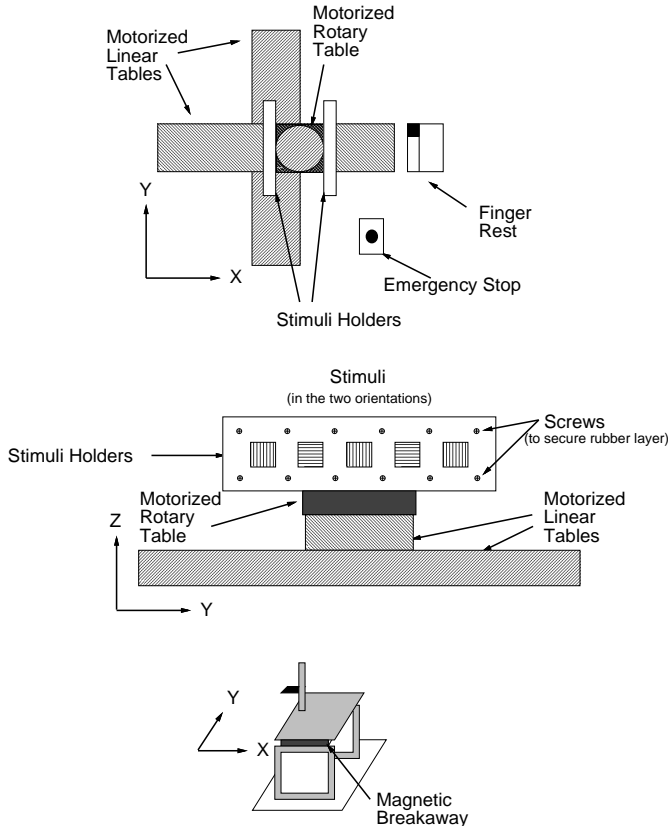


Figure 9: Testing apparatus: a) Top view of overall setup, b) Front view of the tables, stimuli holder, and stimuli, c) Side view of the finger rest

### 3 Experimental Methods

To test the thresholds of human tactile resolution with and without the transmission of shear stress information, we built a system which presents stimuli with different spatial frequencies and orientations and provides easy interchange for two different rubber layers. The system provided accurate position control repeatability.

#### 3.1 Apparatus

We developed a system that allows us to quickly present stimuli patterns to the subject in an accurate manner. The motion control was provided by two motorized linear tables and one motorized rotary table configured in a  $x$ ,  $y$ , and  $\theta$  orientation as shown in Figure 9a. The motorized tables were controlled by a Pentium based PC running Windows NT 4.0. The control program recorded the subjects' responses.

Bolted onto the rotary table were two stimuli holders allowed for 10 stimuli to be used in each experiment (Figure 9b). Wax blocks with horizontal or vertical grating patterns were placed into the holders. The grating patterns had periods ranging from 2.4 mm to 4.8 mm in 0.6 mm increments with a 50% duty cycle. This narrow range of periods was based on the results

of Tan [1995]. The rubber layer was either a solid 2mm silicone rubber sheet or two 1 mm silicone rubber sheets with a thin layer of lubricant in between. We used a vegetable oil spray, PAM<sup>2</sup>, as the lubricant as other lubricants we tried either dried up too quickly or reacted unfavorably with the silicone rubber. The 2 mm thickness for the rubber layer was used based on having an actuator array with 2 mm spacing between the actuators. The 1:1 ratio of spacing and layer thickness gives good anti-aliasing characteristics and signal to noise ratio.

The subject's right index finger was placed in a position such that the presented stimuli would come into contact normally with the fingerpad. It was essential that no extraneous information was given to the subject by having the stimuli contact obliquely and slide across the finger when coming to the final contact position. Two safety devices were incorporated into the design of the system. An emergency stop button was located in an easily accessible place which would immediately stop all motion of the motor tables. The other safety device was a magnetic breakaway located on the finger rest.

#### 3.2 Procedure

Our goal was to measure change in tactile spatial sensitivity without the transmission of shear stress information. Therefore, we designed experiments that measured the threshold of orientation detection with and without the shear stress information.

The experiment consisted of two trials. For the anti-aliasing spatial low-pass filter, one used a solid 2mm silicone rubber sheet and the other used two 1 mm silicone rubber sheets with a thin layer of PAM in between. Which trial was completed first was decided randomly.

In each of the trials, the subject extended their right index finger and placed it on the finger rest (Figure 9c). The finger rest was adjusted to insure that contact with the stimuli would occur in the normal direction of the fingerpad. The control program then allowed the subject to choose how much the stimuli would indent into their finger. The setup was calibrated with a dial indicator to insure that each stimuli would indent to the chosen distance (error of 25  $\mu$ m). The control program then presented each of the ten stimuli fifteen times in a random order. Of the ten stimuli, there were 5 distinct frequencies tested in both orientations. This results in thirty points per frequency tested with half of the points in each orientation. Thirty points per frequency was used because the normal distribution is a good approximation, regardless of the shape of the population, if the sample size is greater than or equal to thirty [Walpole and Myers 1993].

After the control program presents the stimuli, the subject responds with a '0' or '1' corresponding to

<sup>2</sup>American Home Products, Inc.

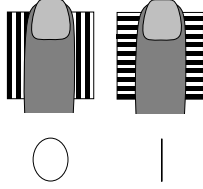


Figure 10: Subjects' response for perceived orientation

Materials	Friction Coeff.
Rubber/wax	1.4
Rubber/Rubber (no lubricant)	2.7
Rubber/Rubber (lubricant)	0.1

Table 1: Measured coefficients of friction

which orientation was felt (Figure 10). The trial was then repeated with the other rubber layer. Each trial took approximately 30 minutes and could be completed on different days, if necessary.

### 3.3 Friction coefficients

We measured friction coefficients between rubber and wax, and two sheets of rubber, with and without the lubricant. A mass was placed on top of the materials being tested. Measuring the horizontal force needed to move the rubber gives the friction coefficient. As shown in Table 1, there is a significant decrease in friction with the lubricant. The low friction between the lubricated layers corresponds to a reduction of  $\tau_{xz}(x, z = d_1)$  applied to the second elastic layer (Figure 4b). Only the normal stress profile,  $\sigma_z(x, z = d_1)$  is transmitted to the second elastic layer.

## 4 Results

The experiments were run on 4 human subjects (3 male, 1 female). All subjects were volunteers, and one subject was familiar with the experimental procedure and apparatus. The subjects' results are shown in Table 2. Graphs of the data are shown in Figure 11. We use 75% correct, the midpoint of chance (50%) and perfect discrimination (100%), as the threshold of perception.

In the shear case, subject 3 did not cross the 75% threshold, and subject 4 could not discriminate the orientation on the 4.8 mm period grating, but was able to on the 4.2 mm grating. In the no shear case, all subjects' discrimination period either improved or stayed the same. The results show that reducing the shear stress information for a static normal stimuli does not deteriorate the perception of orientations. In some subjects, perception of orientations improved at higher frequencies.

Looking at the average of all the subjects (Figure 12), we see that at a 2.4 mm period grating, the percentage correct is approximately chance. As the gratings get more coarse, the percentage correct tends to

Shear					
Period (mm)	2.4	3.0	3.6	4.2	4.8
Subject 1	40	50	77	93	97
Subject 2	67	53	53	73	87
Subject 3	43	47	37	70	73
Subject 4	57	50	57	77	40
Average	51	49	55	78	73

Reduced Shear					
Period (mm)	2.4	3.0	3.6	4.2	4.8
Subject 1	40	70	80	87	100
Subject 2	70	50	50	100	97
Subject 3	67	57	50	100	93
Subject 4	57	90	90	90	100
Average	58	66	67	93	97

Table 2: Raw data from experiments. Numbers are percent correct out of 30 trials per period per subject

increase. In the case without shear information transmission, the percentage correct at 4.2 mm and 4.8 mm period gratings was much higher than the corresponding percentages with shear information.

The experiments of [Tan 1995] studied the frequency at which subjects would perceive a grating. He presented flat and grating patterns to determine at which frequency subjects could discriminate a flat pattern from a grating pattern. The average threshold grating period was 4.0mm. This closely agrees with our results (Figure 12).

## 5 Discussion and Conclusion

The increase in spatial resolution can be best explained by the increase in modulation index for the frequencies of interest (Figure 8). The model predicted an increase in modulation indices, and the experiments verified that at the frequencies tested, the percentage correct was always greater when there was no shear stress information transmitted between the elastic layers.

If we assume that each subject has a threshold period, then the tactile spatial resolution should be improved by reducing the shear stress information. This idea is put to practice in the Sensopad, a device which aids in breast self examinations. It is constructed by placing silicone fluid in between two layers of silicone rubber. Its claim of enhancing the perception of small embedded objects was qualitatively agreed upon, though no quantitative data was taken.

In designing a teletaction system, it is important to consider what type of contacts the sensor will encounter. If the sensor operates in an environment where contact is composed of mainly normal stresses, the reduction of shear stress information can be beneficial by enhancing the higher frequency information present in subsurface skin strain. An example of such

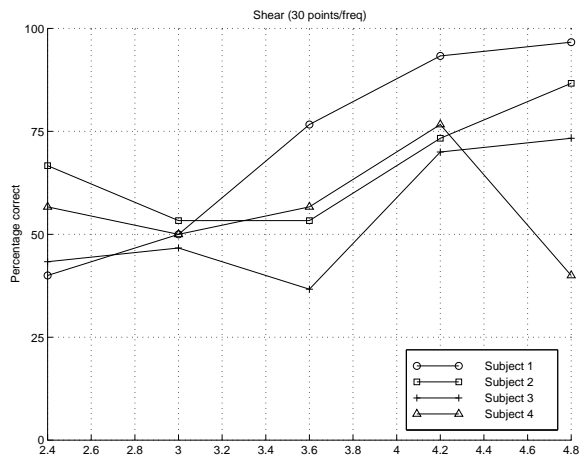


Figure 11: Graphs of the data

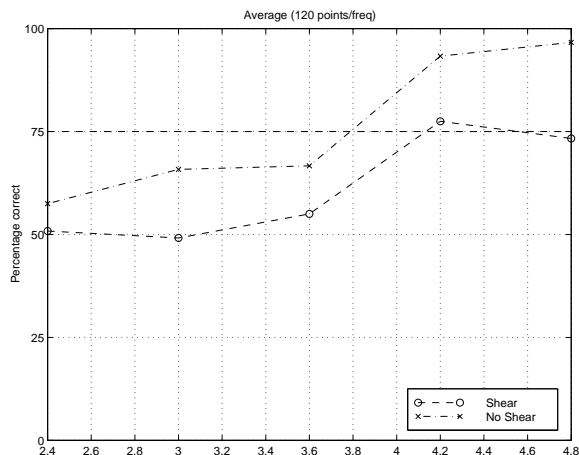


Figure 12: Averages of the data

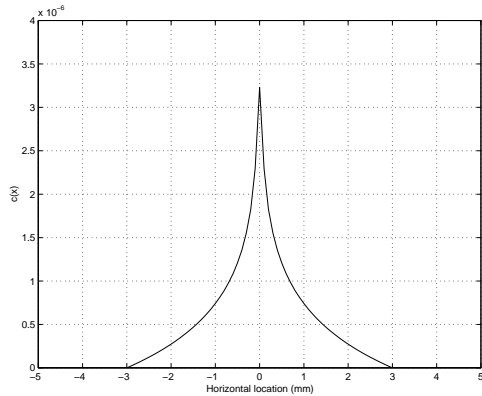


Figure 13: Deflection profile,  $c(x)$ , caused by a line load at  $x = 0$  with  $x_0 = 25\mu m$  and  $x_b = 3.0mm$

an environment is laparoscopic surgery with tactile sensors on the ends of the instruments. Contact with organs will be low friction contacts due to the slipperiness of the organs. This leads to a contact where normal stresses are high when compared to the tangential stresses. In these environments, a tactile display using an array of 1 DOF actuators should be as effective as using an array of 3 DOF actuators.

## 5.1 Future Work

Future work in this area includes allowing the subject to dynamically scan the stimuli, better models of the finger/elastic layer/stimuli interaction, and stimuli with a tangential stress component. Refinement of our apparatus will include integrating a force/torque sensor to give more consistent stimuli presentation.

## Acknowledgments

We thank K. Chiang, J. Yan, W. Zesch, J. Hsu, and A. Mazaheri for helpful discussions and comments.

## Appendix

The fundamental relation between a surface deflection and a normally applied line load is shown in Figure 13 and given by:

$$c(x) = \begin{cases} \frac{2}{\pi E} \log \frac{x_b}{x_o}, & |x| < x_o \\ \frac{2}{\pi E} \log \frac{x_b}{x}, & x_o < |x| < x_b \\ 0, & x_b < |x| \end{cases} \quad (1)$$

where  $x_0$  is half the width of the applied line load, and  $x_b$  is the distant boundary. So from equation 1, the line load has a constant deflection in the width of application, decays logarithmically until the distant boundary, and is zero outside of the distant boundary. We used the values used by [Phillips and Johnson 1981] and [Tan 1997],  $x_0 = 25 \mu m$  and  $x_b = 3mm$ .

As in [Phillips and Johnson 1981], we assume that the deflection is proportional to the magnitude of the

line load, the deflection function,  $c(x)$ , is space invariant, and the overall deflection profile is the superposition of deflection profiles from the individual line loads. Discretizing  $c(x)$ , we can represent the discretized deflection profile  $d(x_i)$  as:

$$d(x_i) = \sum_{j=1}^n c(x_i - x_j)p(x_j) \quad (2)$$

where  $p(x_j)$  is the discretized line load profile, and  $n$  is the number of points representing the profiles. Rewriting equation 2 least squares problem. Given a deflection profile,  $d$  and the deflection matrix,  $C$  (calculated from  $c(x)$ ), we can find  $p$  as follows:

$$Cp = d \quad (3)$$

$$p = (C^T C)^{-1} C^T d \quad (4)$$

In our case,  $p$  and  $d$  are the same length, so

$$p = C^{-1}d \quad (5)$$

## References

- [1] M. Cohn, M. Lam, and R. Fearing, "Tactile Feedback for Teletactile Operation", *SPIE Telemanip. Tech.*, 1833:240-254, 1992.
- [2] R.S. Fearing, G. Moy, E. Tan, "Some Basic Issues in Teletactile", *IEEE Int. Conf. on Rob. and Auto.*, vol. 4, pp 3093-9, Albuquerque, April 1997.
- [3] H. Fischer, B. Neisius, and R. Trapp, "Tactile Feedback for Endoscopic Surgery", *Interactive Technology and New Paradigm for Healthcare*, ed: K. Morgan, R.M. Satava, H.B. Sieburg, R. Mattheus, J.P. Christensen, pp. 114-117, IOS Press 1995.
- [4] C.J. Hasser and M.W. Daniels, "Tactile Feedback with Adaptive Controller for a Force-Reflecting Haptic Display", 15th Southern Biomedical Engineering Conf., pp. 526-533, Dayton, OH, 29-31 March 1996.
- [5] R.D. Howe, W.J. Peine, D.A. Kontarinis, and J.S. Son, "Remote Palpation Technology", *IEEE Eng. in Med. and Bio. Mag.*, pp. 318-323, May/June 1995.
- [6] K.A. Kaczmarek, J.G. Webster, P. Bach-y-Rita, and W.J. Tompkins, "Electrotactile and Vibrotactile Displays for Sensory Substitution Systems", *IEEE Trans. on Bio. Eng.*, 38(1):1-16, January 1991.
- [7] K.L. Johnson, *Contact Mechanics*, Cambridge University Press, 1985.
- [8] Lederman, S.J. 1978. "Heightening tactile impressions of surface texture", *Active Touch*, ed. G. Gordon. Oxford: Pergamon Press, pp. 205-214.
- [9] J.M. Loomis and S.J. Lederman, "Tactual Perception", in *Handbook of Perception and Human Performance*, edited by K.R. Boff, L. Kaufman and J.P. Thomas, pp. 31-1:31-41, John Wiley and Sons: New York, 1986.
- [10] J.R. Phillips and K.O. Johnson, "Tactile Spatial Resolution II. Neural Representation of Bars, Edges, and Gratings in Monkey Primary Afferents", *J. Neurophysiology*, 46(6):1192-1203.
- [11] J.R. Phillips and K.O. Johnson, "Tactile Spatial Resolution III. A Continuum Mechanics Model of Skin Predicting Mechanoreceptor Response to Bars, Edges, and Gratings", *J. Neurophysiology*, 46(6):1204-1225.
- [12] M. Shimojo, M. Shinohara, and Y. Fukui, "Human Shape Recognition Performance for 3D Tactile Display", 1997 IEEE International Conference on Systems, Man, and Cybernetics. p. 3192-7 vol.4. Orlando, FL, USA, 12-15 Oct. 1997.
- [13] U. Singh, "Temporal Characteristics of the Human Finger" Master's Report, Dept of EECS, UC Berkeley, May 1997.
- [14] M.A. Srinivasan and K. Dandekar, "An Investigation of the Mechanics of Tactile Sense Using Two Dimensional Models of the Primate Fingertip" *Jnl. of Biomechanical Engineering (trans. of the ASME)*, vol. 118, pp. 48-55, 1996.
- [15] E. Tan, "Estimating Human Tactile Resolution Limits for Stimulator Design", Master's Report, Dept of EECS, UC Berkeley, May 1995.
- [16] R. Walpole and R. Myers, *Probability and Statistics for Engineers and Scientists*. Macmillan Publishing Company, 1972.